↓ Lecture 10 [16.05.25]

3 | Phases:

With our knowledge from Section 2.1.3 we can now classify the four gapped phases separated by phase transitions at $m = 0, 2, 4$:

- $m < 0$:

  Remember that neither the quantum phase nor the Chern number changes as long as the gap does not close. Hence we can choose a limit in the phase for $m < 0$ that makes the computation of the Chern number particularly simple:

  $\lhd\, m \to -\infty \to \vec{d}(\boldsymbol{k}) \approx -m\vec{e}_z \to C(m < 0) = 0 \to$ Trivial band insulator

  Recall that C counts the skyrmions in the BZ, i.e., how often $\hat{d}(\boldsymbol{k}) = \vec{d}(\boldsymbol{k})/|\vec{d}(\boldsymbol{k})|$ "wraps" around the sphere S^2. But if $\vec{d}$ is pinned to the north pole of S^2, it cannot "wrap" anything.

- $m > 4$:

  $\lhd\, m \to +\infty \to \vec{d}(\boldsymbol{k}) \approx -m\vec{e}_z \to C(m > 0) = 0 \to$ Trivial band insulator

  The argument is the same as for $m < 0$.

- $0 < m < 2$:

  $\lhd$ Transition from $m < 0$ to $m > 0 \to$ Gap closing at $\boldsymbol{\Gamma}$:

  $$H_{\text{QWZ}}(\boldsymbol{\Gamma} + \boldsymbol{k}) = k_x\sigma^x + k_y\sigma^y - m\sigma^z + \mathcal{O}(k^2) \tag{2.44}$$

  Eq. (2.41) $\to$

  $$\begin{aligned} C(0 < m < 2) &= C(m < 0) + \Delta C(m < 0 \to m > 0) && \text{(2.45a)} \\ &= 0 - \left[\frac{\text{sign}(-m)|_{m>0}}{2} - \frac{\text{sign}(-m)|_{m<0}}{2}\right] && \text{(2.45b)} \\ &= +1 && \text{(2.45c)} \end{aligned}$$

  $\to$ Topological phase (I)

- $2 < m < 4$:

  $\lhd$ Transition from $m > 4$ to $m < 4 \to$ Gap closing at $\boldsymbol{M}$:

  $$H_{\text{QWZ}}(\boldsymbol{M} + \boldsymbol{k}) = -k_x\sigma^x - k_y\sigma^y + (4 - m)\sigma^z + \mathcal{O}(k^2) \tag{2.46}$$

  The negative signs of the momenta do not affect the result for the Chern number. You show this on ➲ Problemset 5, see also Eq. (2.60) in Section 2.3 later.

  Eq. (2.41) $\to$

  $$\begin{aligned} C(2 < m < 4) &= C(m > 4) + \Delta C(m > 4 \to m < 4) && \text{(2.47a)} \\ &= 0 - \left[\frac{\text{sign}(4 - m)|_{m<4}}{2} - \frac{\text{sign}(4 - m)|_{m>4}}{2}\right] && \text{(2.47b)} \\ &= -1 && \text{(2.47c)} \end{aligned}$$

  $\to$ Topological phase (II) $\neq$ Topological phase (I)

In summary, this leads us to the …

Phase diagram:

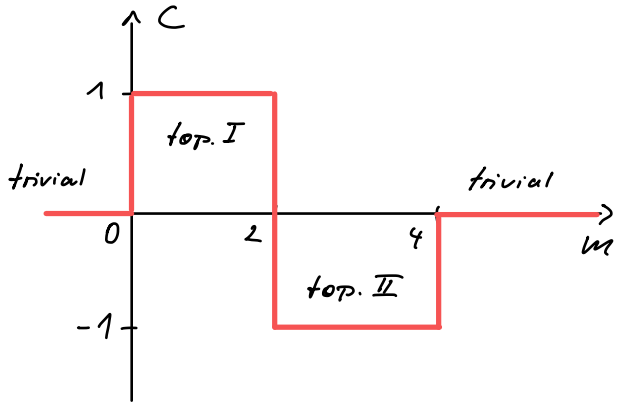

- The two trivial phases for $m < 0$ and $m > 4$ are the *same* trivial quantum phase, i.e., they can be connected by continuously deforming the Hamiltonian without closing the gap. To do this, start from the limit $m \ll 0$ where $\vec{d}$ points to the north pole and then rotate this vector [more precisely: this (almost constant) function] continuously to the south pole (without changing its length). Then you end up in the phase for $m \gg 4$ while the gap on the path was always on the order of $|\vec{d}|$ (i.e., very large).
- By contrast, the two topological phases I and II are *different* quantum phases that cannot be connected by smooth deformations of the Hamiltonian without closing the gap. This follows from the discreteness of the Chern number and the definition of the latter in terms of the normalized Bloch vector $\hat{d}(\boldsymbol{k})$.
- Note that we can compute $C(2 < m < 4)$ alternatively via the transition from $m < 2$ to $m > 2$. At this transition there are *two* Dirac points ($\boldsymbol{X}$ and $\boldsymbol{Y}$), each of which contributes a change of the Chern number by -1 which explains the jump from $C(0 < m < 2) = +1$ to $C(2 < m < 4) = -1$.
- It is highly recommended to plot $\vec{d}(\boldsymbol{k})$ on the BZ as a vector field and observe the changes for $m < 0$ to $m > 4$ (in `Mathematica` you can use the `Manipulate` function to visualize the changes). Try to count the skyrmions, i.e., how often $\vec{d}(\boldsymbol{k})$ "wraps" around the sphere (and in which direction).

4 | Real-space Hamiltonian:

The real-space Hamiltonian of the QWZ model is defined on a square lattice with spin-$\frac{1}{2}$ fermions on the sites (the spin DOF is responsible for the two bands):

i | SP Hilbert space spanned by

$$|\Psi_{i\alpha}\rangle \to \underbrace{|x, y\rangle}_{\text{external}} \otimes \underbrace{|\sigma\rangle}_{\text{internal}} \tag{2.48}$$

$x = 1, \ldots, N_x$: x-position
$y = 1, \ldots, N_y$: y-position
$\sigma = \pm 1$: spin

The Pauli algebra is then represented as follows:

$$\sigma^x = |+1\rangle\langle -1| + |-1\rangle\langle +1| \tag{2.49a}$$
$$\sigma^y = i|-1\rangle\langle +1| - i|+1\rangle\langle -1| \tag{2.49b}$$
$$\sigma^z = |+1\rangle\langle +1| - |-1\rangle\langle -1| \tag{2.49c}$$

ii | SP Hamiltonian:

$$\begin{aligned} H_{\mathrm{QWZ}} \triangleq & -\sum_{x,y}\left[|x+1,y\rangle\langle x,y| \otimes \frac{\sigma^z - i\sigma^x}{2} + \mathrm{h.c.}\right] \\ & -\sum_{x,y}\left[|x,y+1\rangle\langle x,y| \otimes \frac{\sigma^z - i\sigma^y}{2} + \mathrm{h.c.}\right] \\ & -(m-2)\sum_{x,y}|x,y\rangle\langle x,y| \otimes \sigma^z \end{aligned} \tag{2.50}$$

- The kinetic terms of the Hamiltonian (hopping in x- and y-direction) couple the spatial ("orbital") motion with the internal ("spin") degrees of freedom. This is an example of ↓ *spin-orbit coupling* in a lattice model.
- Fourier transform H_{QWZ} in both spatial directions and show that the Bloch Hamiltonian is $H_{\mathrm{QWZ}}(\boldsymbol{k})$ as defined above.

Pictorially:

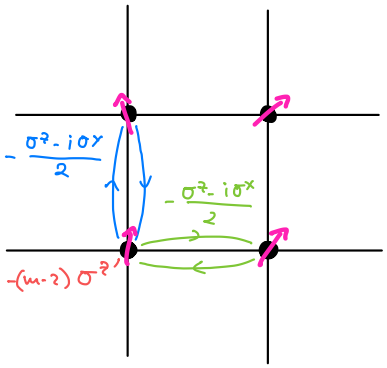

iii | Note that there is no magnetic field involved and therefore no magnetic unit cell necessary.

→ This makes the QWZ model our first Chern insulator! ☺

(For the parameters $0 < m < 2$ or $2 < m < 4$, otherwise it is a trivial band insulator.)

Strictly speaking, we should use the SP Hamiltonian (2.50) to construct via Eq. (2.4) the corresponding second quantized MB Hamiltonian $\hat{H}_{\mathrm{QWZ}}$ that acts on fermionic Fock space. The topological phase is then realized by the *many-body ground state* of $\hat{H}_{\mathrm{QWZ}}$ for $0 < m < 2$ or $2 < m < 4$. This ground state is the Fermi sea obtained by filling the lower of the two bands (both of which are Chern bands; recall that the sum of all Chern numbers always vanishes, ➔ Problemset 3).

2.3. The Haldane Model

- Historically, the Haldane model (HM) on the honeycomb lattice was the first model that realized the phenomenology of the IQHE without (external) magnetic fields (and therefore without Landau levels) [19]; this phenomenon is nowadays referred to as ⁂ *quantum anomalous Hall effect (QAHE)*.
- Hence the Haldane model is also regarded as the prototype of a ← *Chern insulator*. However, some also refer to the ← *Hofstadter model* as a Chern insulator* [35].
- Regarding classification (← Section 0.6), the Haldane model belongs to the same ← *invertible topological order* as the IQHE (← Chapter 1): it features chiral edge modes but no anyonic excitations and is not protected by any symmetry (only quantization of the Hall response requires charge conservation).
- HALDANE discussed this model in his 2016 Nobel Lecture [103].

1 | Rationale of the following construction:

1. Start with the Hamiltonian of ↓ *graphene*:
   → 2 Dirac cones in the BZ (but not gapped!)
2. Add a staggered potential (parameter m) to break the → *sublattice symmetry (SLS)* (→ ??):
   → Gap opens at Dirac points but Chern number is zero since TRS is not broken.
   → Dead end! ☹
3. Add instead a complex next-nearest neighbor (NNN) hopping (strength t and phase φ) to break ← *time-reversal symmetry*:
   → Gap opens at Dirac points *and* Chern number is non-zero.
   → Success! ☺
4. Map out the phase diagram in the m/t-φ plane.

2 | ◁ Real-space MB Hamiltonian on the honeycomb lattice:

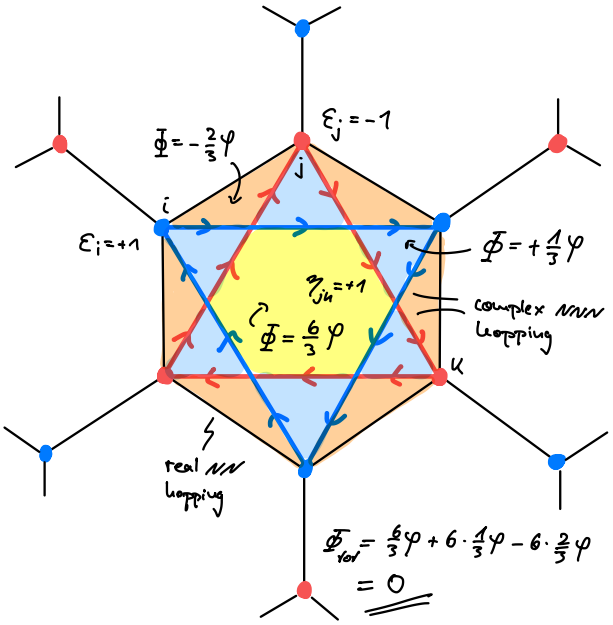

$$\hat{H}_{\mathrm{H}} = \underbrace{\sum_{\langle i,j\rangle} c_i^\dagger c_j}_{\text{Graphene}} + \underbrace{m\sum_i \epsilon_i c_i^\dagger c_i}_{\text{Staggered potential}} + \underbrace{t\sum_{\langle\langle i,j\rangle\rangle} e^{\eta_{ij} i\varphi} c_i^\dagger c_j}_{\text{Complex NNN hopping}} \tag{2.51}$$

- $\langle i, j \rangle$: Nearest-neighbours (NN)
- $\langle\langle i, j \rangle\rangle$: Next-Nearest-neighbours (NNN)
- m: Strength of the staggered potential
- t: Strength of the complex NNN hopping
- φ: Phase of the complex NNN hopping
- $\epsilon_i = \pm 1$: Sublattice-dependent sign (see sketch above)
- $\eta_{ij} = \pm 1$ and $\eta_{ij} = -\eta_{ji}$: Direction-dependent sign
  It is $\eta_{ij} = +1$ ($\eta_{ij} = -1$) if the arrow points from i to j (j to i) in the sketch above.

Notes:

- This is a two-band model because of the two sites in each unit cell of the honeycomb lattice, i.e., the fermions are *spinless*. (This is in contrast to the QWZ model where the two bands described internal spin degrees of freedom.)
- Despite the complex hopping, there is no *net* magnetic flux through the plaquettes of the honeycomb model, $\Phi_{\text{tot}} = 0$, hence no magnetic unit cell is needed (cf. the ← *Hofstadter model*).
- You can think of the complex hoppings arising from a *local* magnetic field "curled up" in each plaquette (maybe due to local magnetic moments in the material):

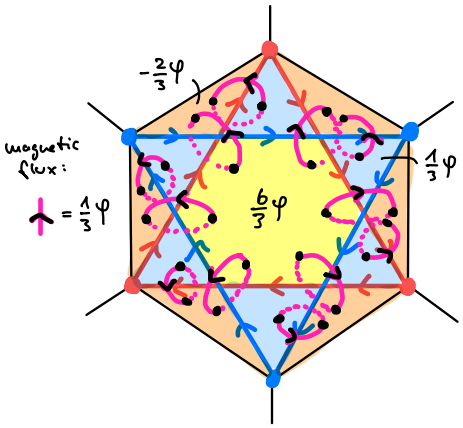

  Note that other equivalent gauges (= distribution of complex hopping phases) are possible. For instance, one can "concentrate" the accumulated phase on the central third of the NNN hopping trajectories so that the outer (orange) triangles do not carry any flux and the blue triangles cancel the flux through the yellow hexagon.
- The staggered potential breaks → *sublattice symmetry* (SLS, **??**) but not ← *time-reversal symmetry* (TRS, Section 2.1.2), whereas the complex NNN hopping breaks SLS *and* TRS. Breaking SLS *and/or* TRS is sufficient to open a gap at the Dirac points, but only breaking of TRS can result in bands with non-zero Chern number.

3 | Momentum space representation of H_{H}:

We want to understand the physics of Eq. (2.51) in momentum space:

i | Brillouin zone:

Honeycomb lattice = Hexagonal/Triangular lattice + 2-atom basis

- Hexagonal lattice → Brillouin zone

- 2-atom basis → 2 bands

Basis vectors of the Hexagonal lattice:

$$\boldsymbol{a}_1 = \frac{1}{2}\left(\sqrt{3}, 1\right)^T \quad \text{and} \quad \boldsymbol{a}_2 = \frac{1}{2}\left(\sqrt{3}, -1\right)^T \tag{2.52}$$

→ Reciprocal lattice (= Hexagonal lattice):

$$\boldsymbol{b}_1 = 2\pi\left(\frac{1}{\sqrt{3}}, 1\right)^T \quad \text{and} \quad \boldsymbol{b}_2 = 2\pi\left(\frac{1}{\sqrt{3}}, -1\right)^T \tag{2.53}$$

The ↓ *reciprocal lattice* is defined by vectors $\boldsymbol{b}$ that satisfy $\boldsymbol{b}\cdot\boldsymbol{a} \in 2\pi\mathbb{Z}$ for $\boldsymbol{a} \in \mathbb{Z}\boldsymbol{a}_1 + \mathbb{Z}\boldsymbol{a}_2$ some lattice vector of the original lattice. The vectors $\boldsymbol{b}_i$ above are a basis of this reciprocal lattice.

→ Brillouin zone = Wigner-Seitz cell of the reciprocal lattice:
(= rotated Honeycomb plaquette)

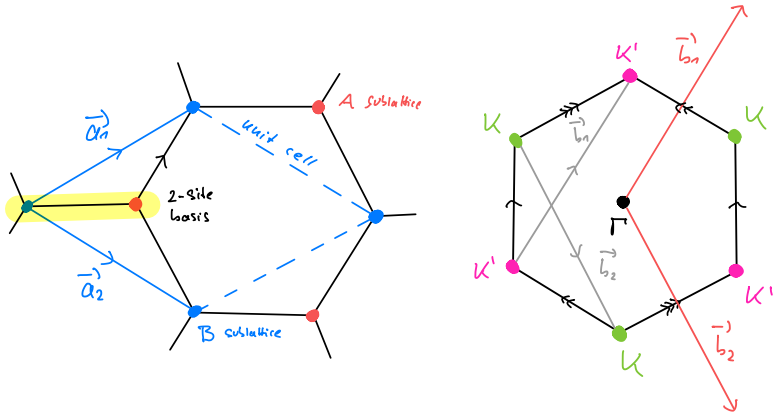

Note that the BZ obtained from the Wigner-Seitz cell is a *torus* T^2 even though this is not obvious from its shape (the BZ of *every* 2D periodic system is a torus as it is just the parallelogram spanned by the reciprocal basis $\boldsymbol{b}_i$ with opposite edges identified):

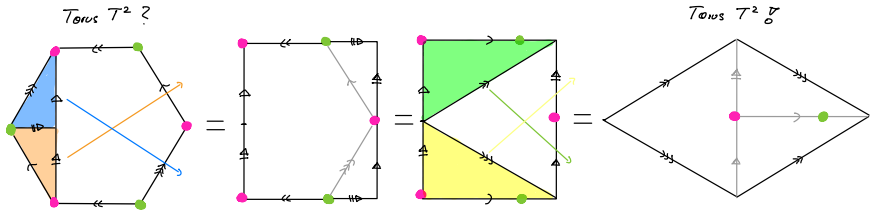

(Edges with the same arrow type are identified along the direction indicated by the arrow.)

The last diagram is known as ↑ *fundamental polygon* of the torus.

ii | Bloch Hamiltonian:

The two sublattice degrees of freedom per unit cell lead to a 2×2 Bloch Hamiltonian $H_{\mathrm{H}}(\boldsymbol{k}) = \varepsilon(\boldsymbol{k})\mathbb{1} + \vec{d}(\boldsymbol{k})\cdot\vec{\sigma}$ with

$$d_x \doteq \cos(\boldsymbol{k}\boldsymbol{a}_1) + \cos(\boldsymbol{k}\boldsymbol{a}_2) + 1 \tag{2.54a}$$
$$d_y \doteq \sin(\boldsymbol{k}\boldsymbol{a}_1) + \sin(\boldsymbol{k}\boldsymbol{a}_2) \tag{2.54b}$$
$$d_z \doteq m + 2t\sin(\varphi)\left[\sin(\boldsymbol{k}\boldsymbol{a}_1) - \sin(\boldsymbol{k}\boldsymbol{a}_2) - \sin(\boldsymbol{k}(\boldsymbol{a}_1 - \boldsymbol{a}_2))\right] \tag{2.54c}$$
$$\varepsilon(\boldsymbol{k}) \doteq 2t\cos(\varphi)\left[\cos(\boldsymbol{k}\boldsymbol{a}_1) + \cos(\boldsymbol{k}\boldsymbol{a}_2) + \cos(\boldsymbol{k}(\boldsymbol{a}_1 - \boldsymbol{a}_2))\right] \tag{2.54d}$$

As $\varepsilon(\boldsymbol{k})$ has no effect on the gap and the Chern number, we set it the following to zero.

The above Bloch Hamiltonian follows straightforwardly from the Hamiltonian Eq. (2.51) together with the sketches above (for the sign conventions) and the Fourier transform

$$c_{x,\boldsymbol{r}} = \frac{1}{\sqrt{L_1 L_2}} \sum_{\boldsymbol{k}\in T^2} e^{-i\boldsymbol{k}\boldsymbol{r}} \tilde{c}_{x,\boldsymbol{k}} \quad \text{and} \quad \tilde{c}_{x,\boldsymbol{k}} = \frac{1}{\sqrt{L_1 L_2}} \sum_{\boldsymbol{r}\in\mathcal{L}} e^{i\boldsymbol{k}\boldsymbol{r}} c_{x,\boldsymbol{r}} \tag{2.55}$$

of the fermion modes on the sublattices $x = A, B$ with $\mathcal{L} = \boldsymbol{a}_1\mathbb{Z}_{L_1} + \boldsymbol{a}_2\mathbb{Z}_{L_2}$ the (periodic) lattice and T^2 the Brillouin zone. It is then

$$\hat{H}_{\mathrm{H}} = \sum_{\boldsymbol{k}\in T^2} \Psi_{\boldsymbol{k}}^\dagger H_{\mathrm{H}}(\boldsymbol{k}) \Psi_{\boldsymbol{k}} \tag{2.56}$$

with $\Psi_{\boldsymbol{k}} = (\tilde{c}_{A,\boldsymbol{k}}, \tilde{c}_{B,\boldsymbol{k}})^T$.

iii | Gap can only close at the corners of the BZ (check this for $m = 0$ and $t = 0$):

$$\boldsymbol{K} \doteq \frac{2\pi}{3}\left(\sqrt{3}, 1\right) \quad \text{and} \quad \boldsymbol{K}' \doteq \frac{2\pi}{3}\left(\sqrt{3}, -1\right) \tag{2.57}$$

For $m = 0$ and $t = 0$ the Hamiltonian Eq. (2.51) describes the ↓ *semimetal* ↓ *Graphene* with two Dirac cones where the two bands touch.

iv | → Dirac Hamiltonians: (Here i, j run only over 1, 2: σ^x and σ^y)

$$H_{\mathrm{H}}(\boldsymbol{K} + \boldsymbol{k}) \doteq k_i h_{ij} \sigma^j + \overbrace{[m - 3\sqrt{3}t\sin(\varphi)]}^{h_z} \sigma^z + \mathcal{O}(k^2) \tag{2.58a}$$

$$\text{with} \quad h = \frac{\sqrt{3}}{2}\begin{bmatrix} 0 & -1 \\ 1 & 0 \end{bmatrix}$$

$$H_{\mathrm{H}}(\boldsymbol{K}' + \boldsymbol{k}) \doteq k_i h'_{ij} \sigma^j + \overbrace{[m + 3\sqrt{3}t\sin(\varphi)]}^{h'_z} \sigma^z + \mathcal{O}(k^2) \tag{2.58b}$$

$$\text{with} \quad h' = \frac{\sqrt{3}}{2}\begin{bmatrix} 0 & -1 \\ -1 & 0 \end{bmatrix}$$

We will use these two Dirac Hamiltonians to derive conditions when the gap closes (= a phase transition occurs) and to compute the Chern numbers of the bands using the tricks developed in Section 2.1.3.

4 | Gap closings:

We start by identifying the parameters where the gap closes to pin down the phase transitions:

$$@\boldsymbol{K}: \quad h_z \overset{!}{=} 0 \quad \Leftrightarrow \quad \frac{m}{3\sqrt{3}t} = +\sin(\varphi) \tag{2.59a}$$

$$@\boldsymbol{K}': \quad h'_z \overset{!}{=} 0 \quad \Leftrightarrow \quad \frac{m}{3\sqrt{3}t} = -\sin(\varphi) \tag{2.59b}$$

→ Preliminiary phase diagram:

Eq. (2.59) suggests to use the ratio $\frac{m}{3\sqrt{3}t}$ of staggering strength m and NNN hopping strength t as an independent parameter:

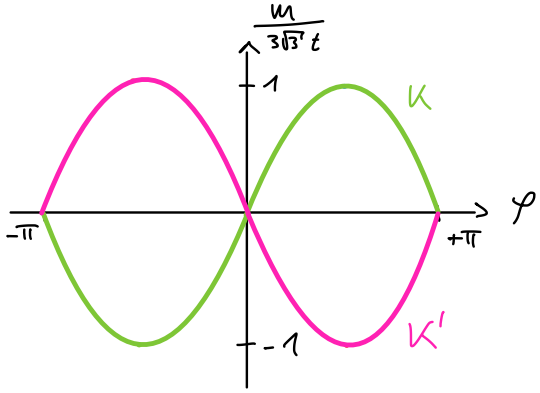

There are 4 different parameter regimes that are separated by lines where the gap closes (note that the two points $\varphi = \pm\pi$ are identified). To identify the phases, we have to compute the Chern number (of the lower band) in all 4 areas …

5 | To do this, we need the following generalized expression for the Chern number of a Dirac Hamiltonian (cf. Section 2.1.3 and our analysis of the QWZ model in Section 2.2):

$$H(\boldsymbol{k}) = \sum_{i,j=1}^{2} k_i h_{ij} \sigma^j + h_z \sigma^z \quad \Rightarrow \quad C = -\frac{\operatorname{sign}(h_z)\operatorname{sign}(\det h)}{2} \tag{2.60}$$

Proof: Problemset 5

Eqs. (2.58) and (2.60) →

$$C_{\boldsymbol{K}} = -\frac{1}{2}\operatorname{sign}[m - 3\sqrt{3}t\sin(\varphi)]\,, \tag{2.61a}$$

$$C_{\boldsymbol{K}'} = +\frac{1}{2}\operatorname{sign}[m + 3\sqrt{3}t\sin(\varphi)]\,. \tag{2.61b}$$

The different sign for $C_{\boldsymbol{K}'}$ is due to $\det h' = -1$.

With these preparations we can finally characterize the four gapped phases …

6 | Phases:

We use the same approach as for the QWZ model in Section 2.2.

- $m \to +\infty$:

$$\vec{d}(\boldsymbol{k}) \overset{2.54}{\approx} m\vec{e}_z \quad \to \quad \text{Trivial phase with } C = 0 \tag{2.62}$$

- $m \to -\infty$:

$$\vec{d}(\boldsymbol{k}) \overset{2.54}{\approx} m\vec{e}_z \quad \to \quad \text{Trivial phase with } C = 0 \tag{2.63}$$

- $0 < \varphi < \pi$ and change parameters as follows:

$$\underbrace{m > 3\sqrt{3}t\sin(\varphi)}_{A} \quad \mapsto \quad \underbrace{m < 3\sqrt{3}t\sin(\varphi)}_{B} \tag{2.64}$$

This means we cross a phase boundary where the gap closes at $\boldsymbol{K}$ →

$$C = 0 + C_{\boldsymbol{K}}(B) - C_{\boldsymbol{K}}(A) \overset{2.61a}{=} [-1/2 \cdot (-1)] - [-1/2 \cdot (+1)] = +1 \tag{2.65}$$

→ Topological phase (I)

- $-\pi < \varphi < 0$ and change parameters as follows: [note that $\sin(\varphi) < 0$]

$$\underbrace{m > -3\sqrt{3}t\,\sin(\varphi)}_{A} \quad \mapsto \quad \underbrace{m < -3\sqrt{3}t\,\sin(\varphi)}_{B} \tag{2.66}$$

This means we cross a phase boundary where the gap closes at $\boldsymbol{K}'$ →

$$C = 0 + C_{\boldsymbol{K}'}(B) - C_{\boldsymbol{K}'}(A) \overset{2.61b}{=} [+1/2 \cdot (-1)] - [+1/2 \cdot (+1)] = -1 \tag{2.67}$$

→ Topological phase (II)

→ Phase diagram:

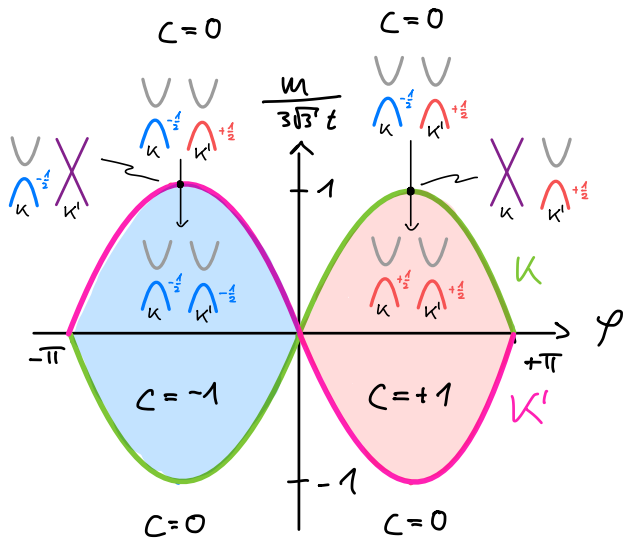

Thus in total ther are *three* different phases, one trivial ($C = 0$) and two topological ($C = \pm 1$). Note that just as for the QWZ model, the two trivial regions with $C = 0$ are continuously connected without closing the gap, i.e., they are *the same phase*.

→ 2 × Topological phases + Trivial phase

7 | Time-reversal symmetry:

Finally, let us check when the model becomes time-reversal symmetric.

◁ $\tilde{T}_0 = \mathcal{K}$ & Eq. (2.34) (assume $t \neq 0$) →

$$d_x(\boldsymbol{k}) \overset{?}{=} d_x(-\boldsymbol{k}) \quad \checkmark \tag{2.68a}$$

$$d_y(\boldsymbol{k}) \overset{?}{=} -d_y(-\boldsymbol{k}) \quad \checkmark \tag{2.68b}$$

$$d_z(\boldsymbol{k}) \overset{?}{=} d_z(-\boldsymbol{k}) \quad \checkmark \text{ for } \varphi = 0, \pi \mod 2\pi \quad \times \text{ otherwise} \tag{2.68c}$$

The spin-$\frac{1}{2}$ TRS representation $\tilde{T}_{\frac{1}{2}} = \sigma^y \mathcal{K}$ is always broken, irrespective of the parameter φ.

→ $C = 0$ for $\varphi = 0, \pi \mod 2\pi$ (i.e., for real NNN hopping)

¡! Note that when TRS is broken for $\varphi \neq 0, \pi \mod 2\pi$, it is only *possible* that $C \neq 0$; the phase diagram above demonstrate that TRS breaking *not* sufficient.

2.4. ‡ Experiments

- In 2010 it was predicted that the QAHE could be observed in certain solid state systems [104], namely magnetic → *topological insulators*.
- These predictions were experimentally confirmed in 2013 [105] and further explored in the following years [106, 107].
- The Haldane model on the honeycomb lattice was artifically realized in a quantum simulator based on ultracold fermions in 2014 [108].
- Much later, in 2023, a quantum simulation with ultracold fermions of the Qi-Wu-Zhang model was reported [109].